The staggered retreat of grounded ice in the Ross Sea, Antarctica since the LGM

Matthew A. Danielson[1], Philip J. Bart[1]

[1]Department of Geology and Geophysics, Louisiana State University, Howe-Russell Geoscience Complex E235, Baton Rouge, LA 70803, USA

Correspondence to: Matthew A. Danielson (mdani38@lsu.edu)

Abstract.

The retreat of the West Antarctic Ice Sheet (WAIS) in the Ross Sea after the LGM was more significant than for any other Antarctic sector. Here we combined the available chronology of retreat with new mapping of seismically resolvable grounding zone wedges (GZWs). Mapping GZWs is important because they record the locations of former stillstands in the extent of grounded ice for individual ice streams during the overall retreat. Our analysis shows that the longest stillstands occurred early in the deglacial and had millennial durations. Stillstands ended abruptly with retreat distances measured in the tens to hundreds of kilometers creating deep embayments in the extent of grounded ice across the Ross Sea. The location of embayments shifted through time. The available chronological data shows that cessation of WAIS and East Antarctic Ice Sheet (EAIS) stillstands were highly asynchronous across at least five thousand years. There was a general shift to shorter stillstands throughout the deglacial. Asynchronous collapse of individual catchments during the deglacial suggests that the Ross Sea sector would have contributed to multiple episodes of relatively small amplitude, sea-level rise as the WAIS and EAIS retreated from the region. The high sinuosity of the modern grounding zone in the Ross Sea suggests that this style of retreat persists.

1 Introduction

By the peak of the Last Glacial Maximum (LGM), grounded ice had advanced to the outermost continental shelf in the western

25 Ross Sea, Antarctica, and to the continental shelf edge in the eastern Ross Sea (Anderson et al., 2014). The extent of grounded

and floating ice was nearly as expansive as it could have been. Six fast flowing ice streams deeply eroded broad, foredeepened

troughs across the continental shelf. Eroded sediment was transported in basal ice and/or subglacially (Alley et al., 1989;

Powell et al., 1996; Alley et al., 2007; Christoffersen et al., 2010; Prothro et al., 2018). The sediment was ultimately deposited

either on the outer continental shelf or upper slope depocenters (Shipp et al., 1999). In the western Ross Sea, foredeepened

30 Drygalski Trough (DT), JOIDES Basin (JB), and Pennell Trough (PT) extend to the continental shelf edge and were eroded

during several successive glacial maxima. The outer parts of these troughs were partly backfilled with large-scale grounding

zone wedges (GZWs) during and/or after the LGM. In the eastern Ross Sea troughs, where ice had reached the continental

shelf edge, large trough-mouth fans were deposited on the upper slope (Mosola and Anderson, 2006). During the post-LGM

retreat, grounding line retreat paused within the outer reaches of the Glomar Challenger Basin (GCB), Whales Deep Basin

35 (WDB) and Little America Basin (LAB), sufficiently long to deposit large GZWs (i.e., several tens of meters thick and tens of

kilometers long) (Mosola and Anderson, 2006; Bart and Owolana, 2012) . The GZW sediment volumes partly reflect durations

of grounding-line stillstands for individual ice streams (Bart and Cone, 2012; Bart and Owolana, 2012; Bart et al., 2017).

Several previous studies have focused on the changing extent of grounded and floating ice and timing of post-LGM retreat

(Conway et al., 1999; Domack et al., 1999; Mosola and Anderson, 2006). Anderson et al. (2014) conducted the last Ross Sea

40 synthesis of seismic stratigraphy and radiocarbon dates. More recently, Halberstadt et al. (2016) conducted a detailed

evaluation of legacy multibeam data and identified GZWs and mega-scale glacial lineations associated with the LGM and

post-LGM GZW stillstands. These stratigraphic data provide abundant evidence as to the progression of WAIS and EAIS

retreat based on stratigraphic superposition. Here we build on the Halberstadt et al. (2016) study of seafloor morphology by

mapping the sediment volume of the GZWs across the six basins of the Ross Sea to evaluate the duration of individual

45 grounding-zone stillstands. Establishing the former durations of GZWs is important to understand the regional scale ice sheet

retreat in the Ross Sea and thus how ice-volume changes from Antarctica contributed to global sea-level in the past. The paleo-perspective also informs our understanding of how additional contraction might proceed and contribute to future sea-level rise.

2 Methods

2.1 Regional seismic grid

50 Our study generated regional stratigraphic correlations of bounding surfaces across 22 surveys of multi- and single-channel reflection seismic data acquired from across the Ross Sea (Supplemental Table 1). The surveys include 510 seismic lines with a total coverage of ~54,000 km. The data are currently stored and maintained at the Antarctic seismic data library system (SDLS) at the Italian National Institute of Oceanography and Applied Geophysics (OGS) and have been used in previous studies such as Perez et al. (2021). Our mapping focused on GZWs interpreted to be of LGM and post-LGM ages,

55 complementing the analyses of seafloor morphology by Halberstadt et al. (2016). The seismic profiles were interpreted in Petrel (Figure 1). The digital data used in this study have been processed prior to being archived at the SDLS. Individual seismic lines were imported as segy files into the software using separate files containing navigation data.
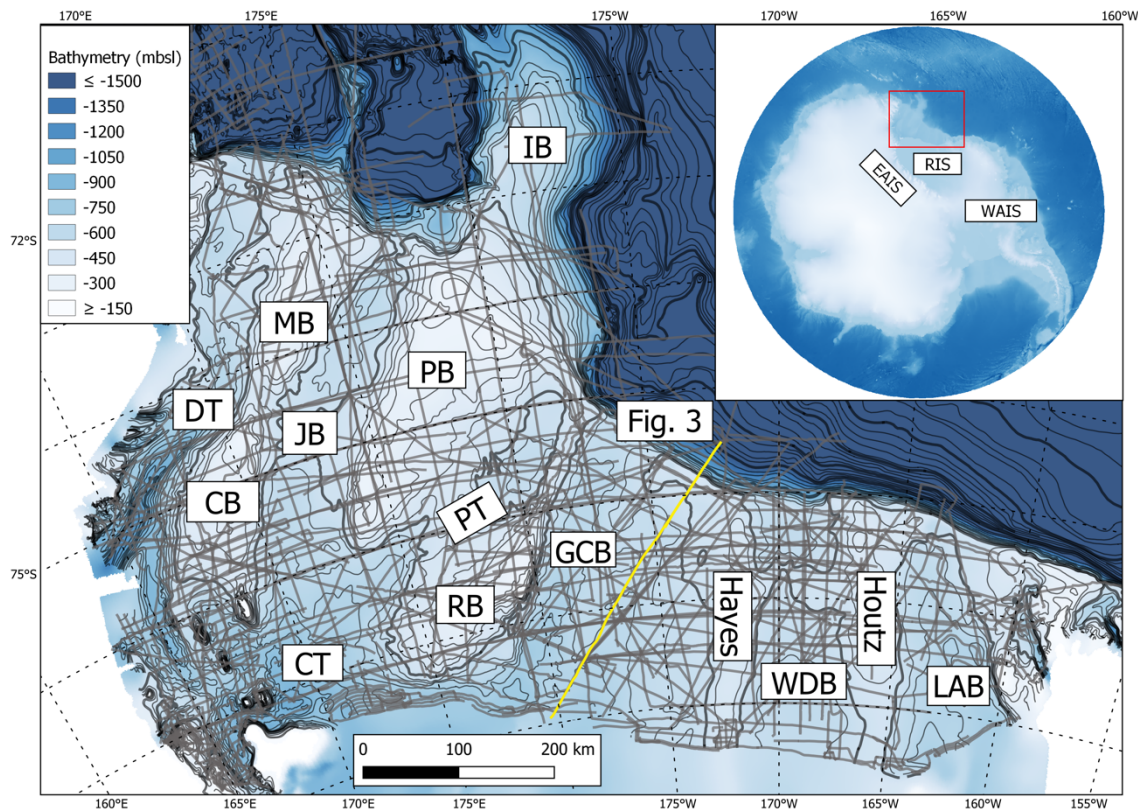
Figure 1: Map of the Ross Sea showing seismic coverage. Bathymetry is from Davey and Nitsche (2013). Inset map of Antarctica using the International Bathymetric Chart of the Southern Ocean ice surface and bathymetry grid showing the locations of the East Antarctic Ice Sheet (EAIS) and the West Antarctic Ice Sheet (WAIS) in addition to the position of the Ross Ice Shelf (RIS) (Dorschel et al., 2022). Main map shows Ross Sea as indicated by the red box on the inset map. Labels of bathymetric troughs on the Ross Sea shelf follow: LAB = Little America Basin, WDB = Whales Deep Basin, GCB = Glomar Challenger Basin, PT = Pennell Trough, CT = Central Trough, JB = JOIDES Basin, DT = Drygalski Trough. Labels of bathymetric banks on the Ross Sea shelf follow: Houtz = Houtz Bank, Hayes = Hayes Bank, RB = Ross Bank, PB = Pennell Bank, IB = Iselin Bank, MB = Mawson Bank, CB = Crary Bank. The position of the Figure 3 seismic profile is indicated with the yellow line.

2.2 Seismic interpretation and isopach mapping of LGM and post-LGM GZWs

We focused on the seismically-resolvable LGM and post-LGM GZWs throughout the Ross Sea that have been identified in

previous seismic studies (Shipp et al., 1999; Mosola and Anderson, 2006; Bart and De Santis, 2012; Bart and Owolana, 2012;

Bart et al., 2017). This includes GZWs identified in legacy multibeam data (Halberstadt et al., 2016). The seafloor reflection

and the unconformities bounding the top and base of the GZWs in each trough on deglaciated Ross Sea shelf were mapped

using regional seismic stratigraphy and comparison to previous studies. Additional single channel paper seismic lines from

four surveys (NBP9307, NBP9401, NBP9501 and NBP9902) were used to supplement the interpretation of major GZW

features. These interpretations were completed on paper and then imported into Petrel using navigation files as a set of points in two-way travel time.

Two-way-travel time maps were made using convergent interpolation in Petrel with a cell size of 50 meters, where the computer-interpreted horizons were the primary input and the paper-interpreted data were secondary input. Time-structure maps were made by subtracting the map of the GZW base from the seafloor map. Refraction sonobuoy measurements in the Ross Sea provide a regional record of sediment velocities (Cochrane et al., 1992; Cochrane et al., 1995). The points of the sonobuoy measurements taken from four expeditions were plotted in Petrel and interpolated to create depth and interval velocity maps. All the analysed GZW deposits were in shallow layers of sediment (upper 250 milliseconds) and thus only the uppermost interval velocity map was used. This section has velocities that vary from 1700 to 2200 meters/second across the region (Supplemental Figure 1). The interval velocity map was then used as an input to build a velocity model in Petrel. Time-structure maps were then depth-converted using the velocity model to create isopach maps for each GZW.

2.3 Volume and duration calculation

The isopach maps were used to calculate sediment volumes for the GZWs in QGIS software. The sediment volumes were then used as a basic parameter to estimate stillstand duration. The paleo-sediment flux for each of the paleo ice streams in the Ross Sea (Equation 1) is defined as Q_s. The paleo-sediment flux of an ice stream is the product of the paleo-drainage area (A) and average sediment yield (S) at the grounding zone where sediment is sourced from upstream subglacial erosion. Our estimates use a simple assumption of the sediment yield and paleo-drainage area. The sediment yield of 0.7 ± 0.21 mm yr^{-1} derived by Bart and Tulaczyk (2020) for the WDB drainage area was applied to the adjacent catchment of LAB to infer a paleo-flux. The 0.7 ± 0.21 mm yr^{-1} sediment yield was derived for the WDB middle shelf GZW which was determined to have been deposited during a stillstand whose onset and cessation dates are constrained by radiocarbon dates (Bart et al., 2018). For the western Ross Sea troughs of PT, JB and DT, we used a sediment yield of 0.49 ± 0.21 mm yr^{-1} which is a value 30% less than the WDB value. This is due to the presence of crystalline and lithified sedimentary bedrock in western Ross Sea (Greenwood et al., 2021). A 30% lower sediment yield would be expected for a catchment floored by crystalline bedrock due to a higher resistance to erosion (Schlunegger et al., 2001). GCB received flow from both East and West Antarctica during the LGM (Licht et al., 2005). Thus, the sediment yield of 0.7 ± 0.21 mm yr^{-1} was used for the parts of the drainage area from West Antarctica (Kamb,

Whillans, Mercer ice streams) and the eastern Ross Sea shelf while the sediment yield of 0.49 ± 0.21 mm yr^{-1}was used for the

100   contribution from the outlet glaciers in East Antarctica such as Beardmore Glacier (Figure 2).

$$Q_s = AS \qquad\qquad\qquad\qquad (1)$$

Paleo-drainage areas were estimated for each of the paleo-troughs of the Ross Sea using the drainage area of the present-day

WAIS ice-streams and EAIS outlet glaciers and projecting their extents into each of the troughs on the outer continental shelf

(Figure 2). The terminus of each paleo-drainage area is the seaward edge of its respective grounding zone wedge. The approach

105   assumes single-ice stream capture for WDB and LAB. The GCB received drainage from the combination of Kamb, Whillans

and Mercer ice streams based on the sub-ice shelf topography shown in the ROSETTA project in addition to other East

Antarctic glaciers (Licht et al., 2005; Tinto et al., 2019). The JB and PT shared capture from Byrd and other smaller East

Antarctic catchments. The upstream drainage area shared by JB and PT was halved for calculations to reflect the shared source

of sediment. DT primarily received ice flow from David Glacier during the LGM (Licht and Palmer, 2013; Licht et al., 2014).

110   There was a reorganization in flow in the southern region of western Ross Sea during the retreat that is marked by backstepping

geomorphological evidence towards David Glacier (Greenwood et al., 2018). Thus, paleo-fluxes for GZWs mapped within the

interior middle shelves of JB were calculated using a modified drainage area from David Glacier with no input from Byrd

Glacier (Figure 2). Grounding duration at each location was calculated using the method following Bart and Tulaczyk (2020)

where ΔT is the grounding duration, V is the total volume of GZW sediment and Q_s is the paleo-sediment flux (Equation 2).

115    $$\Delta T = \frac{V}{Q_s} \qquad\qquad\qquad\qquad (2)$$
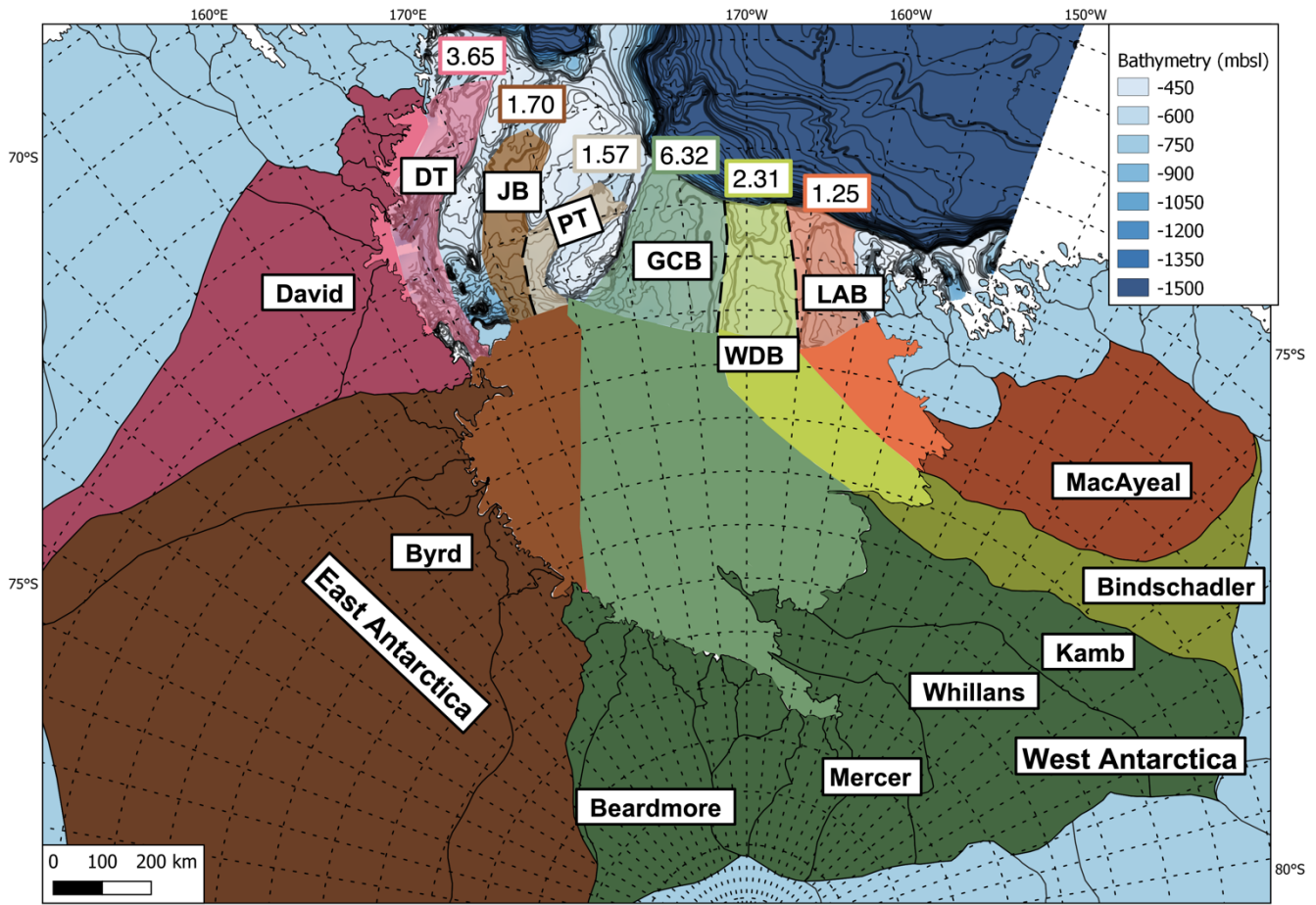
Figure 2: Estimated paleo-drainage catchments for each of the major troughs across the Ross Sea during the LGM. The darker shades correspond with the present-day drainage areas while the lighter shades correspond with the projected paleo-drainage into the troughs when the ice sheet extent was expanded. orange = LAB, yellow= WDB, green = GCB, brown = Pennell and JOIDES, pink = Drygalski Trough. The heavy black dashed line shows the separation between paleo-drainage of adjacent troughs. Drygalski Trough, JOIDES Basin and Pennell Trough capture drainage from East Antarctic glaciers. The upstream drainage area for JOIDES Basin and Pennell Trough is shared with the area upstream of dashed black flow divide being divided by two for the calculations. GCB drained a combination of WAIS paleo-ice streams and EAIS outlet glacier flow. LAB and WDB received sediment from individual WAIS paleo-ice streams. LGM paleo-drainage areas are labeled for each trough where each label is shown in the form of $10^5 km^2$.

3 Results

3.1 Seismic-resolvable GZWs on the Ross Sea shelf

Stratigraphic correlations on the regional seismic transects yielded two-way travel time maps for the Ross Sea outer continental shelf and middle continental shelf (Supplemental Figure 2). The inner continental shelf is covered by the Ross Ice Shelf and

130   hence cannot be investigated using the marine seismic profiles used in this study. Mapped horizons bound GZWs from the base of the LGM unconformity to the seafloor (Figure 3). Seventeen GZWs were identified and mapped within the Ross Sea trough basins (Supplemental Table 3). Fourteen of these GZWs (Figure 4 a-h, k-m, o-q and Table 1) have been identified from previous studies (e.g., Anderson et al., 2013; Halberstadt et al., 2016). Three new GZWs were mapped from the regional seismic data in the inner reaches of the middle continental shelf sectors of JB, PT and GCB (Figure 4 i-j, n; and Table 1). The

135   WDB and PT have two GZWs at the shelf edge and on the middle continental shelf. JB has a GZW at the middle continental shelf and two proximal to the modern ice shelf calving front. in the inner reaches of the trough. The GCB, which has the largest drainage area of all the paleo ice streams, has five GZWs with one at the shelf-edge, one on the middle-shelf and three in the inner reaches of the trough proximal to the modern ice shelf calving front (Table 2; Figure 4).

In the eastern Ross Sea, the shelf edge and outer continental shelf GZWs define part of the modern banks. In the western Ross

140   Sea, the GZWs are trough-confined except for the inner reaches of the middle continental shelf GZWs in DB that were deposited on the banks adjacent to the foredeepened section of the trough (Baroni et al., 2022). Time structure maps were generated for the top and base of each GZW and depth converted. The difference of these two surfaces gives thickness maps for the seventeen GZWs in the Ross Sea (Figure 4).

3.2 Grounding durations of Ross Sea GZWs

145   Sediment volumes for each GZW are shown in Table 1. The outer shelf GZWs in WDB, GCB, JB and DT are the largest with sediment volumes on the order of 10^3 km^3. The inner reaches of the middle continental shelf GZWs have the smallest volumes on the order of 10^2 km^3. The drainage area for the ice streams that deposited these GZWs includes the projected paleo-ice stream drainage pathways (Figure 2) up to the topset-foreset boundary of the mapped GZW. Paleo-flux values are estimated from the product of drainage area with the sediment yield. Stillstand duration was then calculated from the paleo-sediment

150   fluxes and GZW sediment volumes (Tables 2 and 3).

The JB outer continental shelf GZW has the longest duration of ~5.0 kyrs. The inner reaches of the middle continental shelf GZWs in GCB have the shortest durations on the order of 10^1 - 10^2 years. Durations calculations include an uncertainty of ± 2 milliseconds from uncertainty in the TWTT measurement of the GZWs as well as a ± 50 m/s uncertainty from the velocity model used to convert the TWTT maps to depth.
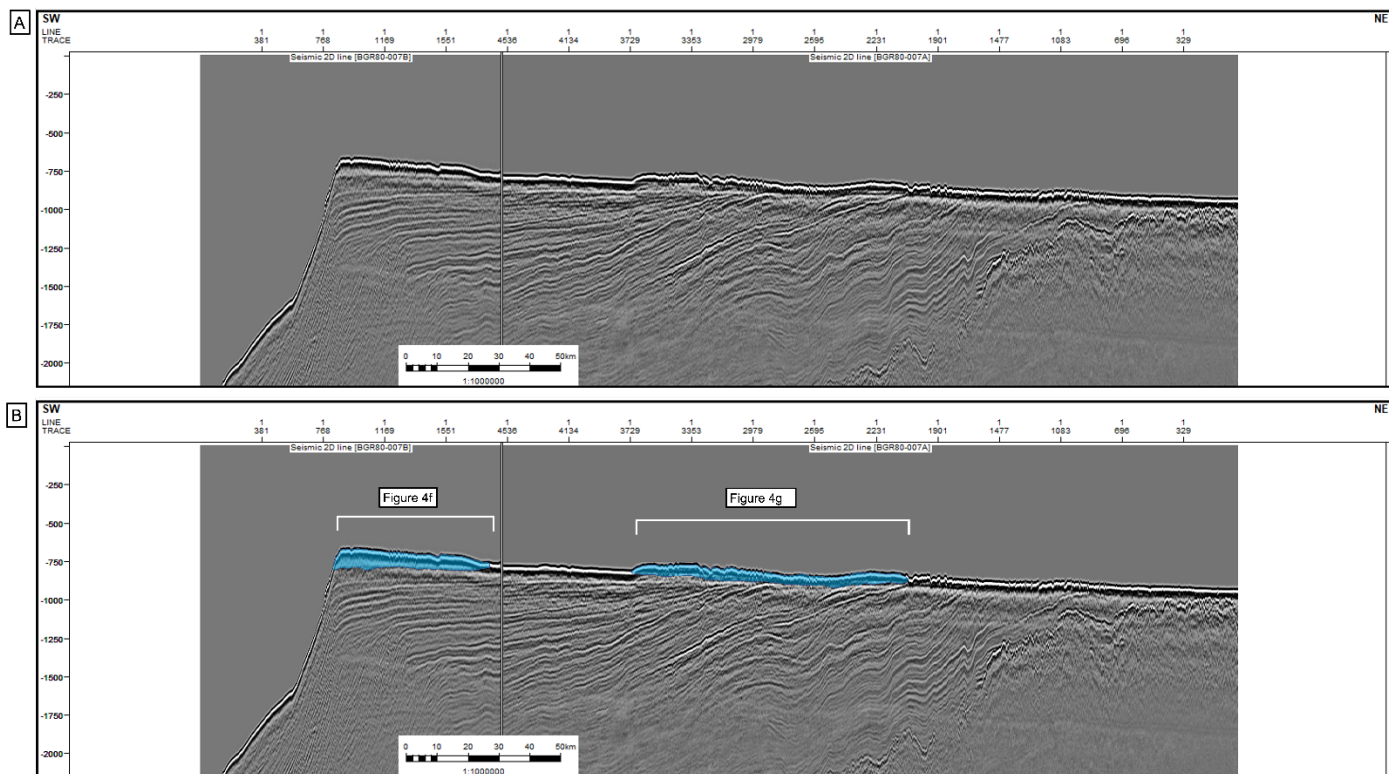
Figure 3: Uninterpreted (A) and interpreted (B) seismic line BGR80-007 through GCB. Location of line is indicated with Figure 1. Blue shaded region shows interpreted GZWs. Position of GZWs and thickness map are shown in Figure 4.

160
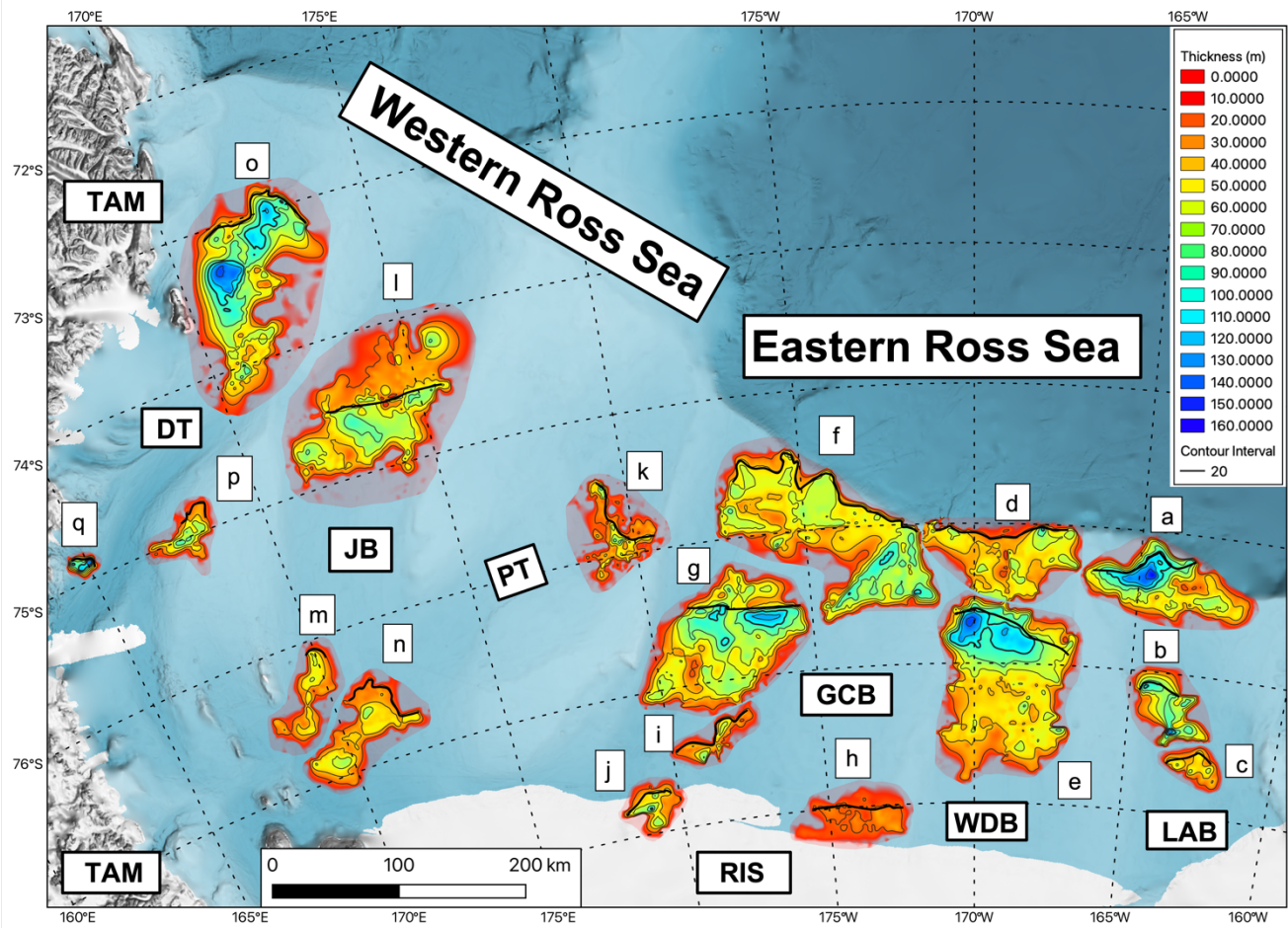
Figure 4: Thicknesses contour maps of Ross Sea GZWs. The heavy black line shows the approximate location of boundary between the GZW topset and foreset. GZWs are labeled "a" to "q" starting in the east with LAB outer shelf GZW. Letter labels of GZWs correspond with records in Table 1. Labels of geometric features follow: LAB = Little America Basin, WDB = Whales Deep Basin, GCB = Glomar Challenger Basin, PT = Pennell Trough, CT = Central Trough, JB = JOIDES Basin, DT = Drygalski Trough, TAM = Transantarctic Mountains, RIS = Ross Ice Shelf. Bathymetry shown in the base map is from IBSCO v2 (Dorschel et al., 2022).. Contour interval = 20 m

GZW Wedge Location	Estimated Paleo Drainage Area, A (10^5 km^2)	GZW Volume, V (km^3)	Paleo Sediment flux, Q (10^8 m^3 a^{-1})	Duration, ΔT (yr)
a. LAB Outer Shelf	1.25	301 ± 19	0.87 ± 0.26	3445 ± 1136
b. LAB Middle Shelf	1.11	120 ± 8	0.79 ± 0.23	1535 ± 506
c. LAB Middle Shelf Inner Reaches	1.05	33 ± 3	0.74 ± 0.22	453 ± 149
d. WDB Outer Shelf	2.31	216 ± 16	1.62 ± 0.49	1027 ± 419
e. WDB Middle Shelf	2.23	534 ± 35	1.67 ± 0.47	3200 ± 700
f. GCB Outer Shelf	6.32	610 ± 41	4.10 ± 1.33	1487 ± 455
g. GCB Middle Shelf West	6.17	523 ± 33	4.00 ± 1.30	1308 ± 399
h. GCB Inner Reaches East	5.80	47 ± 7	3.74 ± 1.22	126 ± 38
i. GCB Inner Reaches West	5.93	33 ± 4	3.83 ± 1.24	87 ± 27
j. GCB Inner Reaches Ross Bank	5.72	45 ± 4	3.68 ± 1.20	121 ± 37
k. PT Middle Shelf	1.57	69 ± 8	0.77 ± 0.34	897 ± 199
l. JOIDES Middle Shelf	1.70	421 ± 37	0.83 ± 0.37	5072 ± 1132
m. JOIDES Inner Reaches 1	0.90	117 ± 11	0.44 ± 0.31	2684 ± 372
n. JOIDES Inner Reaches 2	0.90	58 ± 6	0.44 ± 0.31	1340 ± 186
o. DT Outer Shelf	3.65	583 ± 21	1.79 ± 0.77	3257 ± 752
p. DT Inner Reaches 1	1.17	48 ± 5	0.57 ± 0.68	843 ± 67
q. DT Inner Reaches 2	1.17	20 ± 1	0.57 ± 0.68	350 ± 28

175

Table 1: Summary table of GZWs shown in Figure 4 with drainage area, volume, paleo sediment flux and duration with respective uncertainties.

	Little America	Whales Deep	Glomar Challenger	Pennell	JOIDES	Drygalski
Drainage area ($10^5 \, km^2$)	1.25	2.31	6.32	1.57	1.70	3.65
LGM Paleo-sediment flux ($10^8 \, m^3 \, a^{-1}$)	0.87 ± 0.26	1.62 ± 0.49	4.10 ± 1.33	0.77 ± 0.34	0.83 ± 0.37	1.79 ± 0.77

180

Table 2: Drainage areas and paleo-flux of LGM positions with respective uncertainties.

Shelf position	Little America	Whales Deep	Glomar Challenger	Pennell	JOIDES	Drygalski
1. **outer continental shelf**	301 ± 19	216 ± 16	610 ± 41			583 ± 21
2. **middle continental shelf**	120 ± 8	534 ± 35	523 ± 33	69 ± 8	421 ± 37	
3. inner **middle continental shelf**	33 ± 3		47 ± 7, 45 ± 4, 33 ± 4		117 ± 11, 58 ± 6	48 ± 5, 20 ± 1

Table 3: GZW Volumes (km³) arranged by Ross Sea shelf position with uncertainty.

185

190

4 Discussion

4.1 Stillstand Durations on the Ross Sea continental shelf

4.1.1 Millennial scale stillstand durations on the outer and middle continental shelf

195 We present durations estimated using the sediment yield from the WDB middle continental shelf stillstand for the eastern Ross Sea troughs and a yield that is 30% less for the western Ross Sea troughs. The durations for GCB were calculated using both yields to reflect the drainage from both East and West Antarctica. The calculated durations suggest that the largest GZWs in the Ross Sea had stillstands lasting up to a few millennia (Table 4). This general assessment is strongly supported by radiocarbon dates using benthic foraminifera collected in till of the WDB middle continental shelf stillstand (Bart et al., 2018).

200 The dates suggest that the stillstand had begun by 14.7 ± 0.4 cal kyr BP before retreating by 11.5 ± 0.3 cal kyr BP. The GZWs on the Ross Sea shelf are generally larger than those on other Antarctic continental shelves (Batchelor and Dowdeswell, 2015). In the eastern Ross Sea troughs, larger sediment volumes are partly related to ice stream erosion across the broad West Antarctic catchment areas much of which is underlain by sedimentary bedrock (Tinto et al., 2019). In the Western Ross Sea troughs, there was expanded flow from East Antarctic glaciers through the Transantarctic Mountains during the LGM that

205 provided sediment flux (Licht et al., 2005; Licht and Palmer, 2013). Exposed outcrops in the Transantarctic Mountains suggest that the bedrock that underlaid the expanded flow was primarily crystalline bedrock and metasediments (Li et al., 2020). The high sediment flux and widespread sediment aggradation at the grounding lines (Table 3) would have also contributed to long stillstands by countering the effect of ice-stream thinning associated with the deglaciation as flow accelerates, sea-level rises and global climates warm (Anandakrishnan et al., 2007).

210 **4.1.2 Variable stillstand durations between troughs**

Our data suggest that the grounding line stillstands on the Ross Sea shelf were of millennial and centennial durations. We focus on comparisons to WDB middle continental shelf stillstand because its duration is constrained by radiocarbon dates (Bart et al., 2018). In map view, the WDB middle continental shelf appears to be in regional alignment to the outer continental shelf GZWs in DT and JB, and the middle continental shelf GZWs in PT, GCB, and LAB (Figure 4). Comparison between the

215 middle continental shelf stillstand durations shows that the PT, LAB and GCB stillstand durations are shorter than the WDB stillstand duration. The lower durations for the GCB are a result of a higher paleo-drainage area despite the similar volumes.

The outer continental shelf stillstand in DT has a comparable duration to the WDB stillstand. The middle continental shelf stillstand for the JB has the longest duration of ~5 kyrs.

220

Shelf position	Little America	Whales Deep	Glomar Challenger	Pennell	JOIDES	Drygalski
1. outer continental shelf	3445 ± 1136	1027 ± 419	1487 ± 455			3257 ± 752
2. middle continental shelf	1535 ± 506	3200 ± 700	1308 ± 399	897 ± 199	5072 ± 1132	
3. inner middle continental shelf	453 ± 149		$126 \pm 38, 121 \pm 37, 87 \pm 27$		$2684 \pm 372, 1340 \pm 186$	$843 \pm 67, 350 \pm 28$

Table 4. GZW Durations arranged by Ross Sea shelf position with uncertainty. All durations are presented in years.

4.1.3 Stillstand durations within individual troughs

By stratigraphic superposition, GZWs on the OCS are older than those on the middle continental shelf. Within those basins with more than one GZW, e.g., LAB, our data suggest significant reductions in stillstand durations as the deglacial progressed. The shift to shorter stillstands on the inner reaches of the middle continental shelf is generally consistent with tenets of the marine-ice-sheet-instability hypothesis which predicts unstable grounding line retreat across the foredeepened continental shelf (Weertman, 1974; Joughin and Alley, 2011). Grounding zone deposits that are too small or thin to map with seismic data are reported from several of the Ross Sea shelf troughs from high-resolution swath bathymetry (Halberstadt et al., 2016; Simkins et al., 2017; Greenwood et al., 2018; Bart and Kratochvil, 2022). We follow other studies that suggest these small-scale features would logically correspond to decadal and/or annual timeframes (Livingstone et al., 2016; Dowdeswell et al., 2019).

4.2 Post-LGM erosion rates in the Ross Sea

235 A key assumption of our study is that erosion rates ranged from 0.7 ± 0.21 to 0.49 ± 0.21 mm yr^{-1} for West and East Antarctic catchments respectively. This relatively broad range overlaps with the erosion rate estimates for a modern WAIS ice stream (Alley et al., 1986, 1987). The yields are also within the range of erosion for land-based glaciers from Norway, Svalbard and Switzerland and upper-slope Bear Island trough mouth fan depocenters (Elverhøi et al., 1998). These and other studies show that yield is affected by the degree of ice cover, regional climate, and associated precipitation, and presence/absence of

240 meltwater. All the Ross Sea catchments are south of 70°S and over the post-LGM timeframes we considered, the climates were uniformly colder than present (Cuffey et al., 2016). The catchments were all entirely covered by grounded ice so the degree of glaciation could not have been a significant contributor to erosion rate differences between drainage areas. There is no evidence of warmer-than-present intervals that might have significantly increased meltwater production that would have contributed to high end erosion rates (Cuffey et al., 2016). The lowest erosion rates are expected for large catchments with

245 slow-flowing cold ice (Hallet et al., 1996). Deglacial erosion rates are expected to be high because of the rapid flow of warmer ice (Koppes and Montgomery, 2009; Kingslake et al., 2018).

Additional controls on erosion rates and stillstand durations are subglacial topography, subglacial geology and external atmospheric or oceanographic forcing. Topographic controls on ice stream flow include bottleneck effects from a cross-sectional constriction of trough as well as localized highs of the seafloor (Dowdeswell and Fugelli, 2012; Danielson and Bart,

250 2019; McKenzie et al., 2023). Variations in subglacial geology can also impact erosion rates and stillstand durations where less erodible crystalline and indurated sedimentary bedrock can facilitate longer duration grounding zone deposition (Klages et al., 2015). Bedrock outcropping at the seafloor can decelerate ice sheet retreat and trigger stillstands (Klages et al., 2014). For the GZWs mapped in this study, there was no presence of outcropping bedrock. External climatic forcing is an important control on grounding line stability. Model results suggest that different ocean and atmosphere forcing combinations in the

255 early deglacial are important for controlling the timing and pattern of retreat (Lowry et al., 2020). Changes in the subglacial topography, substrate type, or external climatic forcing could have contributed to variations in erosion rates across the Ross Sea troughs and is reflected in our uncertainty estimates.

All the West Antarctic catchment area is underlain by unconsolidated sediments and sedimentary strata save for small areas of exposed basement (Anderson and Bartek, 1992; Wilson and Luyendyk, 2006; Jordan et al., 2020). Substrates are expected to have similar erodibilities. Thus, the sediment yield of 0.7 ± 0.21 mm yr^{-1} derived by Bart and Tulaczyk (2020) for the WDB drainage area is most appropriate for the eastern Ross Sea troughs of LAB and WDB. The East Antarctic parts of the Ross Sea catchments are underlain by less erodible crystalline rocks and lithified sedimentary bedrock (Greenwood et al., 2021). Yields from basement rock are lower by 30% compared to sedimentary strata (Schlunegger et al., 2001). The sediment yield of 0.49 ± 0.21 mm yr^{-1} is then most appropriate for the western Ross Sea troughs of PT, JB and DT where a less erodible substrate would produce lower average sediment fluxes.

4.3 A staggered post-LGM retreat of grounding lines in the Ross Sea

Grounding line retreat from the DT outer continental shelf stillstand is estimated to have occurred at 16.5 cal kyr BP (Cunningham et al., 1999; Anderson et al., 2014; Prothro et al., 2020). Prothro et al. (2020) used benthic foraminifera from glacial proximal sediments to show that middle shelf grounding zone stillstands in the JB and PT ended at 15.1 cal kyr BP and 13.3 cal kyr BP respectively. Radiocarbon dates from the WDB show that ice had retreated from the shelf edge by 14.7 ± 0.3 cal kyr BP and that retreat from the middle continental shelf occurred at 11.5 ± 0.3 cal kyr BP (Bart et al., 2018). Bart and Cone (2012) proposed the GCB stillstand ended at 27.5 cal kyr BP. A pre-LGM retreat is precluded because data presented by Halberstadt et al. (2016) require that ice remained grounded in both GCB and LAB until after a grounding line embayment opened in the WDB at 11.5 cal kyr BP (Bart and Kratochvil, 2022). The oldest date from deglacial sediment overlying the foreset of the middle continental shelf GZW in GCB requires that the stillstand had ended by 8.7 cal kyr BP (Bart and Cone, 2012). We apply the same age of retreat (8.7 cal kyr) to the LAB middle continental shelf stillstand because the only other radiocarbon ages are from core tops.

Our data do not support previous studies that suggested that retreat occurred in a gradual lockstep fashion (Conway et al., 1999). Instead, both the chronology and stillstand duration data suggest that grounding line retreat proceeded in an unsteady episodic retreat style within individual troughs (Table 5 and Figure 5). The earliest retreat in DT may be partly related to the greater depth of the DT. The subsequent opening of an embayment in PT may have been related to its small catchment area that delivered relatively low volumes of ice to the grounding zone. The sustained grounding in the JB may have been associated

with both its larger catchment, flow capture from the PT catchment and buttressing from its adjacent broad shallow banks. The long stillstand duration in the WDB may have been aided by antecedent topography that includes a bottleneck constriction at

285 the location of the middle continental shelf grounding stillstand (Danielson and Bart, 2019) plus the apparent rapid sediment aggradation following ice shelf break up at 12.3 cal kyr BP (Bart and Tulaczyk, 2020). The available age control (see above) suggests that up to three millennia may have elapsed before grounded ice retreated from the GCB and LABs but here the chronologies are poorly constrained.

We acknowledge that the retreat chronology is likely to change as more radiocarbon data are generated. With the available

290 constraints, our data supports other previous studies that suggested that retreat was not synchronous or in lock step between troughs (Mosola and Anderson, 2006; Halberstadt et al., 2016; Prothro et al., 2020). Neither the onset, duration or termination of Ross Sea stillstands appear to be related to global or regional scale forcing mechanism with the possible exception of the WDB middle continental shelf stillstand which may be bracketed between intervals of rapid, large amplitude sea level rise at meltwater pulses (MWPs) 1a and 1b (Lin et al., 2021). These data are not consistent with the view that WAIS and EAIS

295 contraction in the Ross Sea contributed significantly to the sustained sea-level rise during either MWP1a or 1b. An asynchronous opening of grounding-line embayments would have been associated with multiple episodes of short-lived accelerated sea-level rise. The marked sinuosity of the modern grounding line in the Ross Sea suggests that this staggered retreat persists through to present.

300

GZW Wedge Location	Retreat mode Duration, ΔT (yr)	Nearest retreat date (cal yr BP)	Grounding start date (cal yr BP)	Date Reference
b. LAB Middle Shelf	1535	$8715_b \pm 70$	10250 ± 70	NBP0802 PC2 7 - 9 cm (Bart and Cone, 2012)

e. WDB Middle Shelf	3200	$11500_b \pm 300$	14701 ± 300	NBP1502B KC07 (Bart et al., 2018)
g. GCB Middle Shelf West	1308	$8715_b \pm 50$	10023 ± 50	NBP0802 PC2 7 - 9 cm (Bart and Cone, 2012)
k. PT Middle Shelf	897	$15121_b \pm 270$	16019 ± 270	NBP1502A KC17 144 – 145 cm (Prothro et al., 2020)
l. JOIDES Middle Shelf	5072	$13315_a \pm 240$	18387 ± 240	NBP1502A KC48 Prothro et al., 2020
o. DT Outer Shelf	3257	$16519_b \pm 260$	19776 ± 260	NBP9501 KC37 (Prothro et al., 2020; Anderson 2014; Cunningham et al., 1999)

a: AIO bulk sediment date

b: Benthic carbonate material from grounding zone sedimentation

305 **Table 5: Grounding start date model for the middle continental shelf GZWs.**
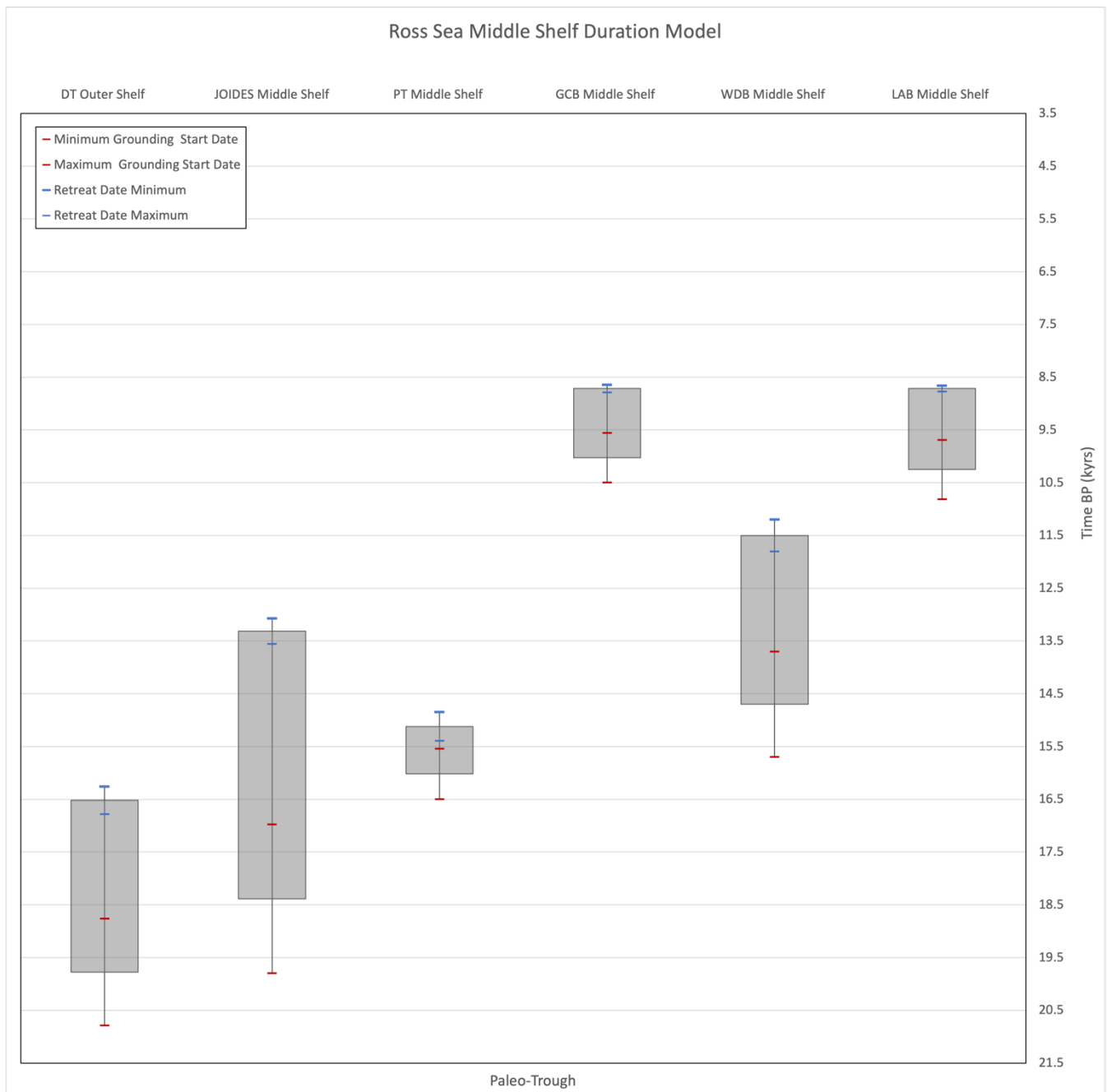
Figure 5. Duration age model for the middle continental shelf GZWs in the Ross Sea using the durations and nearest retreat date plotted in Table 5. The grey box shows the median grounding zone retreat date added to the estimated duration to yield a grounding start date. Blue markers show the uncertainty of the retreat date. Red markers show the uncertainty of the retreat date added to the

duration yielding minimum and maximum grounding start dates. The uncertainty of the duration estimates is incorporated in the minimum and maximum start dates.

5 Conclusion

315   Given the inherent uncertainties in our approach, we acknowledge that future work should focus on more directly constraining onset, duration, and cessation of grounding zone stillstands with radiocarbon data. With the available chronologic data, seismic mapping of GZWs provide reasonable first-order estimates for stillstand duration. The locations and sediment volumes of GZWs suggest millennial to centennial duration stillstands for Ross Sea ice streams during the early phases of the post-LGM retreat followed by a shift to significantly shorter stillstands. Combined with the available age control, our first-order duration

320   estimates strongly suggest a staggered retreat that formed deep grounding-line embayments between troughs. These results can be used as inputs to ice sheet models to better contributions to the post-LGM sea-level rise as the deglacial progressed in the Ross Sea. Asynchronous collapse of individual catchments occurring over the course of the post-LGM suggests that the Ross Sea sector contributed to multiple episodes of relatively small-amplitude sea-level rise rather than fewer intervals of rapid large-amplitude sea level from a regionally synchronous retreat. The high sinuosity of the modern grounding zone in Ross Sea

325   suggests that this retreat style persists.

Data Availability

The data that support the findings of this study are openly available in the SDLS hosted at OGS at
https://sdls.ogs.trieste.it/cache/index.jsp. A full list of seismic surveys used in this study are listed in Supplemental Table 1.

330

Author contribution

MD performed the mapping of the seismic data and figure generation; MD and PB interpreted the results.; MD and PB wrote and edited the manuscript.

335   **Competing interests**

The authors declare that they have no conflict of interest.

Acknowledgments

Support for the project was provided by a United States National Science Foundation Office of Polar Programs Antarctic Earth

340 Sciences Division grant (#1841136) to Bart. Seismic data used for this project were accessed from the Antarctic Seismic Data

Library System (SDLS) hosted at the National Institute of Oceanography and Applied Geophysics (OGS). We thank the

original collectors of these data. A full list of the seismic surveys used can be found in supplemental table 1.

References

345

Alley, R. B., Anandakrishnan, S., Dupont, T. K., Parizek, B. R., and Pollard, D., 2007, Effect of Sedimentation on Ice-Sheet Grounding-Line Stability: Science Reports, v. 315, p. 1838 - 1840.

350 Alley, R. B., Blankenship, D. D., Bentley, C. R., and Rooney, S. T., 1986, Deformation of till beneath ice stream B, West Antarctica: Letters to Nature, v. 322, p. 57-59.

Alley, R. B., Blankenship, D. D., Bentley, C. R., and Rooney, S. T., 1987, Till beneath ice stream B: 3. Till deformation: Evidence and implications: Journal of Geophysical Research, v. 92, no. B9, 10.1029/JB092iB09p08921.

Alley, R. B., Blankenship, D. D., Rooney, S. T., and Bentley, C. R., 1989, Sedimentation beneath ice shelves - the view from ice stream B.:

355 Marine Geology, v. 85, no. 2-4, p. 101-120.

Anandakrishnan, S., Catania, G. A., Alley, R. B., and Horgan, H. J., 2007, Discovery of Till Deposition at the Grounding Line of Whillans Ice Stream: Science Reports, v. 315, p. 1835 - 1837.

Anderson, J. B., and Bartek, L. R., 1992, Cenozoic Glacial History of the Ross Sea Revealed by Intermediate Resolution Seismic Reflection Data Combined with Drill Site Information, The Antarctic Paleoenvironment: A Perspective on Global Change: Part One, p. 231-

360 264.

Anderson, J. B., Conway, H., Bart, P. J., Witus, A. E., Greenwood, S. L., McKay, R. M., Hall, B. L., Ackert, R. P., Licht, K., Jakobsson, M., and Stone, J. O., 2014, Ross Sea paleo-ice sheet drainage and deglacial history during and since the LGM: Quaternary Science Reviews, v. 100, p. 31-54, 10.1016/j.quascirev.2013.08.020.

Baroni, C., Tenti, M., Bart, P., Salvatore, M. C., Gasperini, L., Busetti, M., Sauli, C., Stucchi, E. M., and Tognarelli, A., 2022, Antarctic Ice

365 Sheet re-advance during the Antarctic Cold Reversal identified in the Western Ross Sea: GEOGRAFIA FISICA E DINAMICA QUATERNARIA, v. 45, p. 3-18.

Bart, P., and De Santis, L., 2012, Glacial Intensification During the Neogene: A Review of Seismic Stratigraphic Evidence from the Ross Sea, Antarctica, Continental Shelf: Oceanography, v. 25, no. 3, p. 166-183, 10.5670/oceanog.2012.92.

Bart, P. J., and Cone, A. N., 2012, Early stall of West Antarctic Ice Sheet advance on the eastern Ross Sea middle shelf followed by retreat

370 at 27,50014CyrBP: Palaeogeography, Palaeoclimatology, Palaeoecology, v. 335-336, p. 52-60, 10.1016/j.palaeo.2011.08.007.

Bart, P. J., DeCesare, M., Rosenheim, B. E., Majewski, W., and McGlannan, A., 2018, A centuries-long delay between a paleo-ice-shelf collapse and grounding-line retreat in the Whales Deep Basin, eastern Ross Sea, Antarctica: Sci Rep, v. 8, no. 1, p. 12392, 10.1038/s41598-018-29911-8.

Bart, P. J., and Kratochvil, M., 2022, A paleo-perspective on West Antarctic Ice Sheet retreat: Sci Rep, v. 12, no. 1, p. 17693,

375 10.1038/s41598-022-22450-3.

Bart, P. J., Krogmeier, B. J., Bart, M. P., and Tulaczyk, S., 2017, The paradox of a long grounding during West Antarctic Ice Sheet retreat in Ross Sea: Sci Rep, v. 7, no. 1, p. 1262, 10.1038/s41598-017-01329-8.

Bart, P. J., and Owolana, B., 2012, On the duration of West Antarctic Ice Sheet grounding events in Ross Sea during the Quaternary: Quaternary Science Reviews, v. 47, p. 101-115, 10.1016/j.quascirev.2012.04.023.

380   Bart, P. J., and Tulaczyk, S., 2020, A significant acceleration of ice volume discharge preceded a major retreat of a West Antarctic paleo–ice stream: Geology, v. 48, no. 4, p. 313-317, 10.1130/g46916.1.

Batchelor, C. L., and Dowdeswell, J. A., 2015, Ice-sheet grounding-zone wedges (GZWs) on high-latitude continental margins: Marine Geology, v. 363, p. 65-92, 10.1016/j.margeo.2015.02.001.

Christoffersen, P., Tulaczyk, S., and Behar, A., 2010, Basal ice sequences in Antarctic ice stream: Exposure of past hydrologic conditions
385   and a principal mode of sediment transfer: Journal of Geophysical Research, v. 115, no. F3, 10.1029/2009jf001430.

Cochrane, G. R., Cooper, A. K., Childs, J. R., and Hart, P. E., 1992, USGS seismic refraction surveys in the Ross Sea, 1984-1990: USGS Openfile Reports, v. 92-556.

Cochrane, G. R., De Santis, L., and Cooper, A. K., 1995, Seismic velocity expression of glacial sedimentary rocks beneath the Ross Sea from sonobuoy seismic-refraction data: Geology and Seismic Stratigraphy of the Antarctic Margin: Antarctic Research Series, v.
390   68, p. 261 - 270.

Conway, H., Hall, B. L., Denton, G. H., Gades, A. M., and Waddington, E. D., 1999, Past and Future Grounding-Line Retreat of the West Antarctic Ice Sheet: Science, v. 286, no. 5438, p. 280-283, 10.1126/science.286.5438.280.

Cuffey, K. M., Clow, G. D., Steig, E. J., Buizert, C., Fudge, T. J., Koutnik, M., Waddington, E. D., Alley, R. B., and Severinghaus, J. P.,
        2016, Deglacial temperature history of West Antarctica: Proc Natl Acad Sci U S A, v. 113, no. 50, p. 14249-14254,
395   10.1073/pnas.1609132113.

Cunningham, W. L., Leventer, A., Andrews, J. T., Jennings, A. E., and Licht, K. J., 1999, Late Pleistocene-Holocene marine conditions in the Ross Sea, Antarctica: evidence from the diatom record: The Holocene, v. 9, no. 2, p. 129-139, 10.1191/095968399675624796.

Danielson, M., and Bart, P. J., 2019, Topographic control on the post-LGM grounding zone locations of the West Antarctic Ice Sheet in the Whales Deep Basin, Eastern Ross Sea: Marine Geology, v. 407, p. 248-260, 10.1016/j.margeo.2018.11.001.

400   Domack, E. W., Jacobson, E. A., Shipp, S., and Anderson, J. B., 1999, Late Pleistocene–Holocene retreat of the West Antarctic Ice-Sheet system in the Ross Sea: Part 2—Sedimentologic and stratigraphic signature: Geological Society of America Bulletin, v. 111, no. 10, p. 1517–1536.

Dorschel, B., Hehemann, L., Viquerat, S., Warnke, F., Dreutter, S., Tenberge, Y. S., Accettella, D., An, L., Barrios, F., Bazhenova, E., Black, J., Bohoyo, F., Davey, C., De Santis, L., Dotti, C. E., Fremand, A. C., Fretwell, P. T., Gales, J. A., Gao, J., Gasperini, L.,
405   Greenbaum, J. S., Jencks, J. H., Hogan, K., Hong, J. K., Jakobsson, M., Jensen, L., Kool, J., Larin, S., Larter, R. D., Leitchenkov, G., Loubrieu, B., Mackay, K., Mayer, L., Millan, R., Morlighem, M., Navidad, F., Nitsche, F. O., Nogi, Y., Pertuisot, C., Post, A. L., Pritchard, H. D., Purser, A., Rebesco, M., Rignot, E., Roberts, J. L., Rovere, M., Ryzhov, I., Sauli, C., Schmitt, T., Silvano, A., Smith, J., Snaith, H., Tate, A. J., Tinto, K., Vandenbossche, P., Weatherall, P., Wintersteller, P., Yang, C., Zhang, T., and Arndt, J. E., 2022, The International Bathymetric Chart of the Southern Ocean Version 2: Sci Data, v. 9, no. 1, p. 275, 10.1038/s41597-
410   022-01366-7.

Dowdeswell, J. A., and Fugelli, E. M. G., 2012, The seismic architecture and geometry of grounding-zone wedges formed at the marine margins of past ice sheets: Geological Society of America Bulletin, v. 124, no. 11-12, p. 1750-1761, 10.1130/b30628.1.

Dowdeswell, J. A., Hogan, K. A., and Le Heron, D. P., 2019, The glacier-influenced marine record on high-latitude continental margins: synergies between modern, Quaternary and ancient evidence: Geological Society, London, Special Publications, v. 475, no. 1, p.
415   261-279, 10.1144/sp475.13.

Elverhøi, A., Hooke, R. L., and Solheim, A., 1998, LATE CENOZOIC EROSION AND SEDIMENT YIELD FROM THE SVALBARDÐBARENTS SEA REGION: IMPLICATIONS FOR UNDERSTANDING EROSION OF GLACIERIZED BASINS: Quaternary Science Reviews, v. 17, p. 209 - 241.

Greenwood, S. L., Simkins, L. M., Halberstadt, A. R. W., Prothro, L. O., and Anderson, J. B., 2018, Holocene reconfiguration and readvance
420   of the East Antarctic Ice Sheet: Nat Commun, v. 9, no. 1, p. 3176, 10.1038/s41467-018-05625-3.

Greenwood, S. L., Simkins, L. M., Winsborrow, M. C. M., and Bjarnadóttir, L. R., 2021, Exceptions to bed-controlled ice sheet flow and retreat
from glaciated continental margins worldwide: Science Advances, v. 7, p. 1 - 12.

Halberstadt, A. R. W., Simkins, L. M., Greenwood, S. L., and Anderson, J. B., 2016, Past ice-sheet behaviour: retreat scenarios and changing
425   controls in the Ross Sea, Antarctica: The Cryosphere, v. 10, no. 3, p. 1003-1020, 10.5194/tc-10-1003-2016.

Hallet, B., Hunter, L., and Bogen, J., 1996, Rates of erosion and sediment evacuation by glaciers: A review
of field data and their implications Global and Planetary Change, v. 12, p. 213 -235.

Jordan, T. A., Riley, T. R., and Siddoway, C. S., 2020, The geological history and evolution of West Antarctica: Nature Reviews Earth & Environment, v. 1, no. 2, p. 117-133, 10.1038/s43017-019-0013-6.

430   Joughin, I., and Alley, R. B., 2011, Stability of the West Antarctic ice sheet in a warming world: Nature Geoscience, v. 4, no. 8, p. 506-513, 10.1038/ngeo1194.

Kingslake, J., Scherer, R. P., Albrecht, T., Coenen, J., Powell, R. D., Reese, R., Stansell, N. D., Tulaczyk, S., Wearing, M. G., and Whitehouse, P. L., 2018, Extensive retreat and re-advance of the West Antarctic Ice Sheet during the Holocene: Nature, v. 558, no. 7710, p. 430-434, 10.1038/s41586-018-0208-x.

Klages, J. P., Kuhn, G., Graham, A. G. C., Hillenbrand, C. D., Smith, J. A., Nitsche, F. O., Larter, R. D., and Gohl, K., 2015, Palaeo-ice stream pathways and retreat style in the easternmost Amundsen Sea Embayment, West Antarctica, revealed by combined multibeam bathymetric and seismic data: Geomorphology, v. 245, p. 207-222, 10.1016/j.geomorph.2015.05.020.

Klages, J. P., Kuhn, G., Hillenbrand, C. D., Graham, A. G. C., Smith, J. A., Larter, R. D., Gohl, K., and Wacker, L., 2014, Retreat of the West Antarctic Ice Sheet from the western Amundsen Sea shelf at a pre- or early LGM stage: Quaternary Science Reviews, v. 91, p. 1-15, 10.1016/j.quascirev.2014.02.017.

Koppes, M. N., and Montgomery, D. R., 2009, The relative efficacy of fluvial and glacial erosion over modern to orogenic timescales: Nature Geoscience, v. 2, no. 9, p. 644-647, 10.1038/ngeo616.

Li, X., Zattin, M., and Olivetti, V., 2020, Apatite Fission Track Signatures of the Ross Sea Ice Flows During the Last Glacial Maximum: Geochemistry, Geophysics, Geosystems, v. 21, no. 10, 10.1029/2019gc008749.

Licht, K. J., Hennessy, A. J., and Welke, B. M., 2014, The U-Pb detrital zircon signature of West Antarctic ice stream tills in the Ross embayment, with implications for Last Glacial Maximum ice flow reconstructions: Antarctic Science, v. 26, no. 6, p. 687-697, 10.1017/s0954102014000315.

Licht, K. J., Lederer, J. R., and Jeffrey Swope, R., 2005, Provenance of LGM glacial till (sand fraction) across the Ross embayment, Antarctica: Quaternary Science Reviews, v. 24, no. 12-13, p. 1499-1520, 10.1016/j.quascirev.2004.10.017.

Licht, K. J., and Palmer, E. F., 2013, Erosion and transport by Byrd Glacier, Antarctica during the Last Glacial Maximum: Quaternary Science Reviews, v. 62, p. 32-48, 10.1016/j.quascirev.2012.11.017.

Lin, Y., Hibbert, F. D., Whitehouse, P. L., Woodroffe, S. A., Purcell, A., Shennan, I., and Bradley, S. L., 2021, A reconciled solution of Meltwater Pulse 1A sources using sea-level fingerprinting: Nat Commun, v. 12, no. 1, p. 2015, 10.1038/s41467-021-21990-y.

Livingstone, S. J., Stokes, C. R., Ó Cofaigh, C., Hillenbrand, C.-D., Vieli, A., Jamieson, S. S. R., Spagnolo, M., and Dowdeswell, J. A., 2016, Subglacial processes on an Antarctic ice stream bed. 1: Sediment transport and bedform genesis inferred from marine geophysical data: Journal of Glaciology, v. 62, no. 232, p. 270-284, 10.1017/jog.2016.18.

Lowry, D. P., Golledge, N. R., Bertler, N. A. N., Jones, R. S., McKay, R., and Stutz, J., 2020, Geologic controls on ice sheet sensitivity to deglacial climate forcing in the Ross Embayment, Antarctica: Quaternary Science Advances, v. 1, 10.1016/j.qsa.2020.100002.

McKenzie, M. A., Miller, L. E., Slawson, J. S., MacKie, E. J., and Wang, S., 2023, Differential impact of isolated topographic bumps on ice sheet flow and subglacial processes: The Cryosphere, v. 17, no. 6, p. 2477-2486, 10.5194/tc-17-2477-2023.

Mosola, A. B., and Anderson, J. B., 2006, Expansion and rapid retreat of the West Antarctic Ice Sheet in eastern Ross Sea: possible consequence of over-extended ice streams?: Quaternary Science Reviews, v. 25, no. 17-18, p. 2177-2196, 10.1016/j.quascirev.2005.12.013.

Powell, R. D., Dawber, M., McInnes, J. N., and Pyne, A. R., 1996, Observations of the grounding-line area at a floating glacier terminus: Annals of Glaciology, v. 22, p. 217-223, 10.3189/1996AoG22-1-217-223.

Prothro, L. O., Majewski, W., Yokoyama, Y., Simkins, L. M., Anderson, J. B., Yamane, M., Miyairi, Y., and Ohkouchi, N., 2020, Timing and pathways of East Antarctic Ice Sheet retreat: Quaternary Science Reviews, v. 230, 10.1016/j.quascirev.2020.106166.

Prothro, L. O., Simkins, L. M., Majewski, W., and Anderson, J. B., 2018, Glacial retreat patterns and processes determined from integrated sedimentology and geomorphology records: Marine Geology, v. 395, p. 104-119, 10.1016/j.margeo.2017.09.012.

Schlunegger, F., Melzer, J., and Tucker, G., 2001, Climate, exposed source-rock lithologies, crustal uplift and surface erosion: a theoretical analysis calibrated with data from the Alps/North Alpine Foreland Basin system: International Journal of Earth Sciences, v. 90, no. 3, p. 484-499, 10.1007/s005310100174.

Shipp, S., Anderson, J., and Domack, E., 1999, Late Pleistocene–Holocene retreat of the West Antarctic Ice-Sheet system in the Ross Sea: Part 1—Geophysical results: Geological Society of America Bulletin, v. 111, no. 10, 10.1130/0016-7606(1999)111<1486:Lphrot>2.3.Co;2.

Simkins, L. M., Anderson, J. B., Greenwood, S. L., Gonnermann, H. M., Prothro, L. O., Halberstadt, A. R. W., Stearns, L. A., Pollard, D., and DeConto, R. M., 2017, Anatomy of a meltwater drainage system beneath the ancestral East Antarctic ice sheet: Nature Geoscience, v. 10, no. 9, p. 691-697, 10.1038/ngeo3012.

Tinto, K. J., Padman, L., Siddoway, C. S., Springer, S. R., Fricker, H. A., Das, I., Caratori Tontini, F., Porter, D. F., Frearson, N. P., Howard, S. L., Siegfried, M. R., Mosbeux, C., Becker, M. K., Bertinato, C., Boghosian, A., Brady, N., Burton, B. L., Chu, W., Cordero, S. I., Dhakal, T., Dong, L., Gustafson, C. D., Keeshin, S., Locke, C., Lockett, A., O'Brien, G., Spergel, J. J., Starke, S. E., Tankersley, M., Wearing, M. G., and Bell, R. E., 2019, Ross Ice Shelf response to climate driven by the tectonic imprint on seafloor bathymetry: Nature Geoscience, v. 12, no. 6, p. 441-449, 10.1038/s41561-019-0370-2.

Weertman, J., 1974, Stability of the Junction of an Ice Sheet and an Ice Shelf: Journal of Glaciology, v. 13, no. 67, p. 3-11, 10.3189/s0022143000023327.

Wilson, D. S., and Luyendyk, B. P., 2006, Bedrock platforms within the Ross Embayment, West Antarctica: Hypotheses for ice sheet history, wave erosion, Cenozoic extension, and thermal subsidence: Geochemistry, Geophysics, Geosystems, v. 7, no. 12, p. n/a-n/a, 10.1029/2006gc001294.